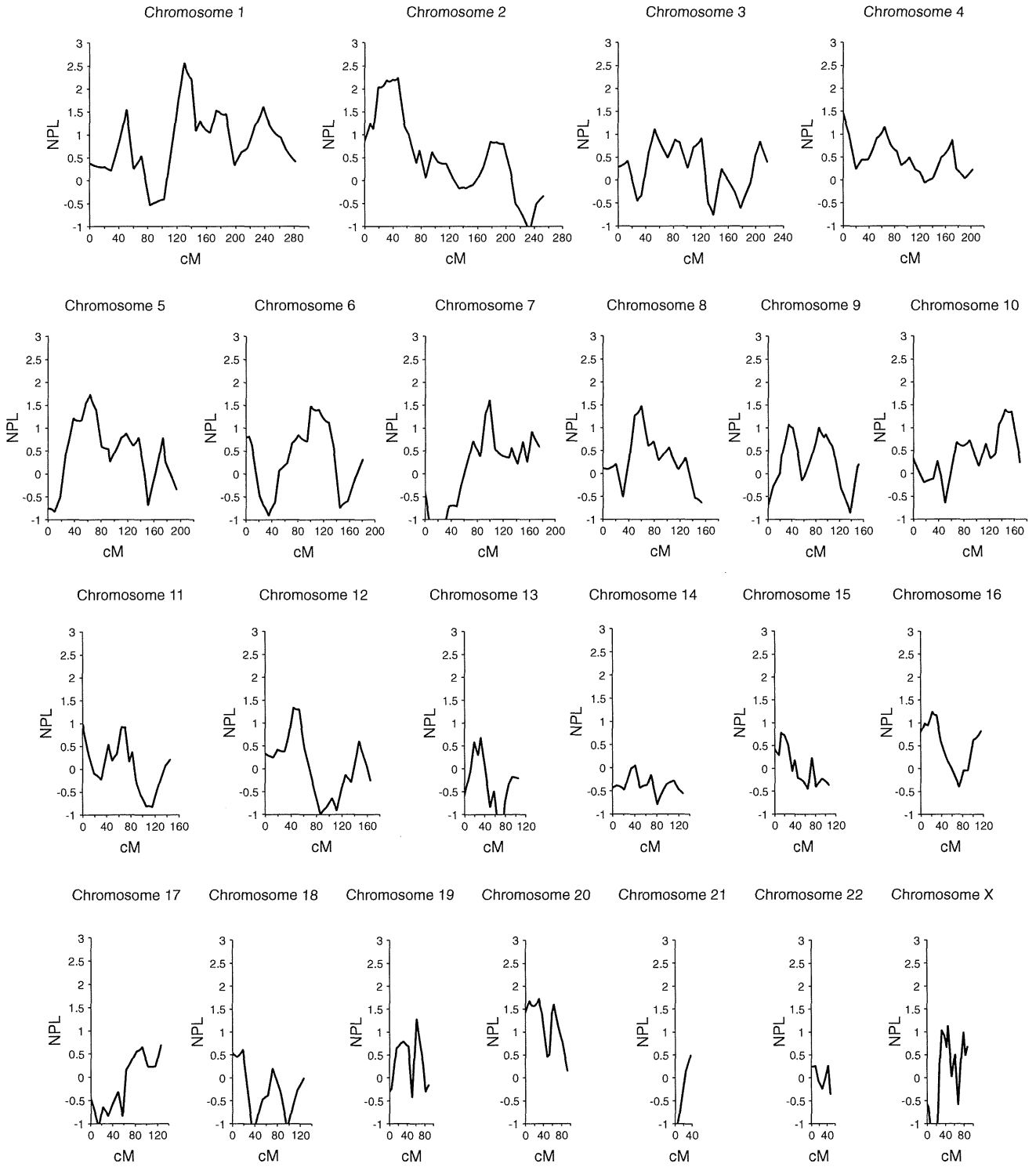

Fig. 1 A genome-wide linkage analysis of ossification of the posterior longitudinal ligament of the spine (OPLL) with definite cervical lesions (ossification more than two vertebral segments). The genotype data of micro-satellite markers for 154 affected sib-pairs were calculated by GENEHUNTER 2.1 for autosomal chromosomes and GENEHUNTER 1.3 for chromosome X. The *x*-axis indicates the genetic distance from the first micro-satellite locus in each chromosome. The *y*-axis indicates the non-parametric linkage (NPL) score values

http://togodb.dbcls.jp/heterozygosity_jp). Primers used for amplification of these markers are available upon request. Allele frequencies of the markers were determined using 92 unrelated non-OPLL subjects. All subjects were >48 years of age and had no signs of OPLL by magnetic resonance imaging.

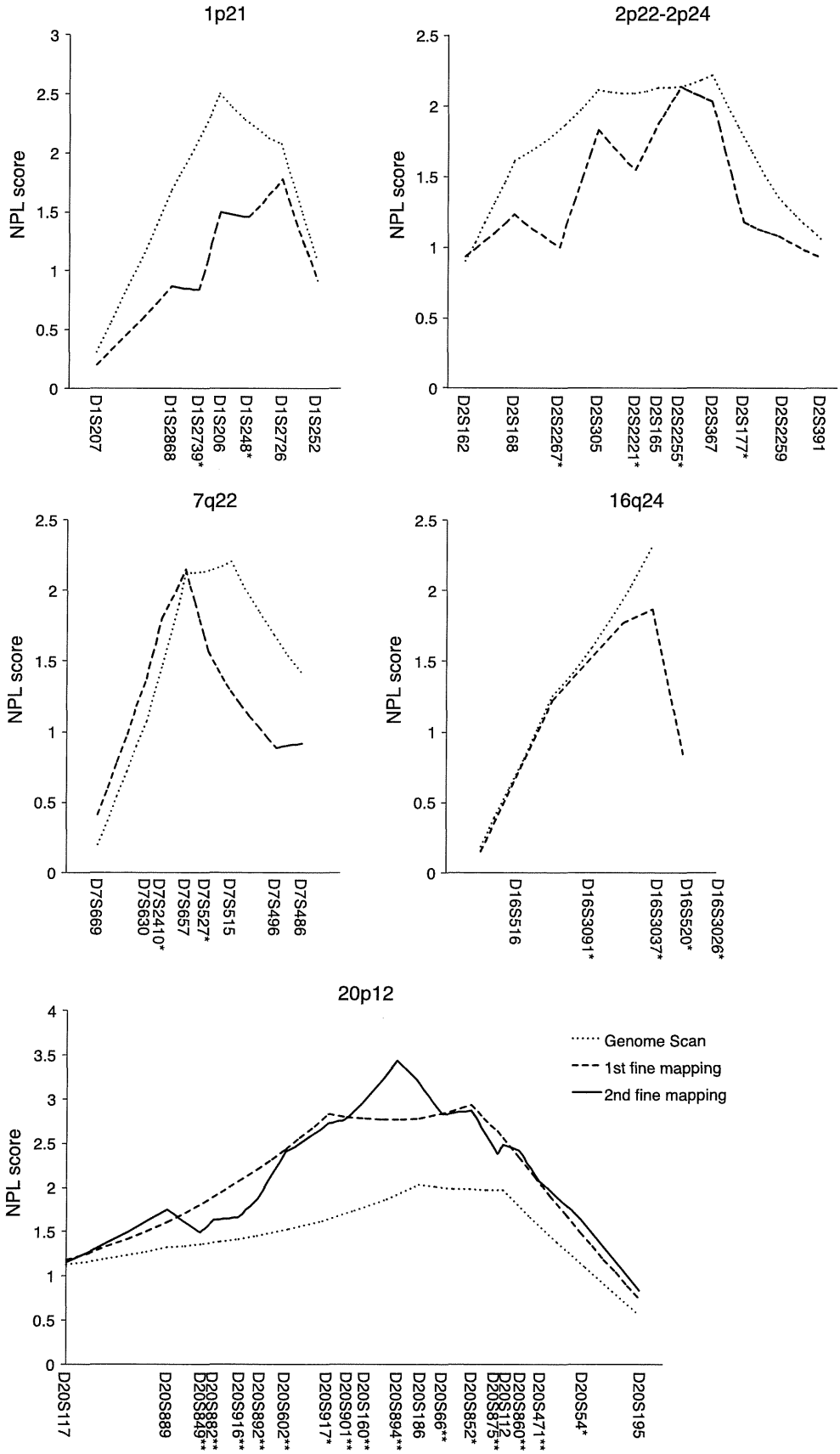

Fig. 2 Fine mapping of chromosome 1p21 and 2p22–2p24 for sib-pairs with definite cervical spine OPLL, 7q22 and 20p12 for non-diabetes mellitus (DM) sib-pairs, and 16q24 for sib-pairs below age 65 years at diagnosis. The genotyped data of microsatellites for affected sib-pairs after stratification were calculated by GENEHUNTER 2.1. Multipoint NPL score curves in the regions on chromosome 1p21, 2p22–2p24, 7q22, 16q24 and 20p12 were plotted. *Single and double asterisks* indicate the markers in the first and second fine mapping marker sets, respectively

Statistical analysis

Multipoint non-parametric linkage (NPL) analysis of the data was performed using the GENEHUNTER 2.1 program [25] for autosomal chromosomes and the GENEHUNTER 1.3 program for chromosome X. The identity by descent (IBD) was calculated and information content was estimated. NPL scores and *P* values were calculated to assess the statistical evidence for linkage. Allele frequencies of micro-satellite markers were estimated in 64 unrelated Japanese subjects [22].

Results

The DNAs were obtained with clinical information from a total of 410 OPLL subjects (Table 1), which consisted of 214 affected sib pairs from 196 Japanese families. Among the 406 markers genotyped, three markers (D14S68, D6S446 and DXS8067) were excluded from the linkage analysis because of insufficient data. Furthermore, 11 markers (D1S214, D1S2836, D2S396, D4S414, D6S262, D7S486, D7S2465, D17S921, D18S70, D20S192 and D20S196) were excluded, because they had insertion and deletion polymorphisms around their di-nucleotide repeat sequences. The average genotyping success rate of the 392 markers was 97.4 %. There was no evidence of suggestive linkage (defined as NPL score >2.2) [26]. A maximum NPL score of 1.99 ($P = 0.023$) was obtained near marker D7S657. The NPL scores for all autosomes and X chromosome are available upon request.

OPLL is a heterogeneous disorder and phenotypic stratification could possibly reduce the heterogeneity. We selected subjects having definite cervical OPLL, i.e., cervical OPLL of more than two vertebral segments, because cervical OPLL is the predominant type and small cervical OPLL is sometime difficult to distinguish from other conditions including spondyloarthritis. A total of 297 subjects comprising 154 pairs were included in the subgroup (Table 1). The NPL scores for all autosomes and X chromosome are shown in Fig. 1. Four chromosomal regions showed *P* values <0.05. Among them, three markers in two chromosomal regions showed evidence of suggestive linkage (Table 1). The most significant linkage was found on chromosome 1p21 with a maximum NPL score of 2.55 ($P = 0.005$) near marker D1S206.

Several clinical factors including age [27], DM [28] and obesity [29] have been reported as risk factors for OPLL. To further reduce the potential heterogeneity of OPLL, we stratified the subjects by age at a diagnosis of OPLL, DM, obesity estimated by BMI and the severity of OPLL (number of ossified vertebrae).

We first stratified the subjects based on OPLL severity defined by the number of ossified cervical vertebra of more than three. The number of sib-pairs of the subgroup decreased to 89; however, the maximum NPL score on 2p22–2p24 increased to 2.65 at D2S165 in this severe OPLL group (Table 1), while significance of the linkage on 1p21 decreased (NPL score 1.32).

For stratified analysis by age, sib-pairs below age 65 years at diagnosis were selected among the definite cervical OPLL pairs, because saturation of trend in age-specific cervical OPLL incidence rate at 60–69 years old is reported [27]. The subgroup composed of 74 pair with relatively younger age of onset is expected to be under stronger genetic influence. The genome-wide linkage analysis on the non-elderly subgroup showed a new evidence of linkage on 16q24 (Table 1). Other loci did not show suggestive linkage.

The third stratification group consisted of sib-pairs without DM (103 sib-pairs). Again, in spite of marked decrease of the number of pairs, the NPL score on 1p21 was increased to 2.64 at D1S206. In addition, two new scores as evidence of linkage were found on 7q22 (NPL score 2.21) and 20p12 (NPL score 2.21) (Table 1). A stratified analysis based on obesity, which was composed of non-obese 115 sib-pairs, showed no evidence of linkage. Plots of NPL scores for all stratified analyses are available upon request.

We then performed fine mapping by including markers around the peaks of 1p21 and 2p22–2p24 loci, which were identified by linkage analysis of definite cervical spine OPLL subjects and around those of 7q22, 16q24 and 20p12 loci, which were identified in further stratification analyses. The fine mapping showed the best evidence of linkage on 20p12, with a maximum NPL score of 2.93 near marker D20S852 (Fig. 2). NPL scores of the other loci decreased under the threshold for suggestive linkage. Further addition of 12 markers around the peak of 20p12 with an average interval of 2 cM detected the highest NPL score (3.43, $P = 0.00027$) at D20S894 (Fig. 2).

Discussion

We collected as many as 410 samples that went far beyond previous OPLL linkage studies. Past three linkage studies reported *COL11A2* (6p21) [30], *COL6A1* (21q21) [8], and *BMP4* (14q22–q23) [11] as OPLL susceptibility genes; however, those studies had only 124, 169, and 172 samples. In addition, most of the subjects were collected in very limited areas in a northern and a southern district of Japan. We collected samples from all over Japan and, hence, there is little possibility of region specific sampling bias. Although previous association studies reported more than a

dozen of genes as candidate genes for OPLL, all did not show any evidence of linkage in our study.

We consider that the failure of our initial analysis to find the linked region might be partly due to heterogeneity of OPLL. To avoid diagnostic heterogeneity of OPLL, we adopted stricter inclusion criteria. It is suggested that inclusion criteria with more severe phenotypes could facilitate the genomic study of disease-susceptibility genes by organizing genetically more homogeneous group [31]. In spite of the significant decrease of numbers of the samples (214–154 pairs), stratification by excluding ambiguous subjects lead to identification of linked loci with suggestive linkage. Further stratification by three previously recognized confounding factors lead to increase linkage score in 2 of 3 already identified loci and identification of 3 new loci with suggestive linkage, again in spite of an even more significant decrease of numbers of the samples (154 to <103 pairs).

A stratified analysis based on the absence of complication of DM in cervical OPLL, and subsequent fine mapping analysis identified the best evidence of linkage on 20p12. Insulin has been implicated in bone formation [32]. Abnormal insulin metabolism often complicates OPLL; high OPLL prevalence has been reported in non-insulin-dependent DM [33]. Therefore, different etiology could be expected between subgroups with/without DM, justifying our stratification. The linkage region (1-LOD support interval of the linkage peak) spanned 9.3 Mb and contained 25 known genes. Jagged 1 (*JAG1*) in the region could be a good candidate gene for OPLL, because of its potential involvement in the enchondral bone formation. *JAG1* belongs to the Delta/Serrate domain (DSL) family, which is the ligand for the receptor, Notch. *JAG1* is expressed in osteoblastic cells in vivo and in vitro. Jagged 1-activated Notch 1 signal is involved with increased bone mineral deposition [34]. Association of a functional SNP in *JAG1* with the bone mineral density has been reported [35]. An association study using SNPs is necessary to determine whether effects of this locus on OPLL susceptibility result from JAG1. Although it was out of the 1-LOD support interval of the linkage peak, bone morphogenetic protein 2 (BMP2) in the region also could be a candidate gene for OPLL. The BMP2 has been implicated as an important regulator of bone metabolism. The BMP2 and BMP2 mRNA are overexpressed in ossifying matrix and chondrocytes adjacent to cartilaginous areas of OPLL tissues [36, 37].

Genetic and environmental factors involved in the etiology and pathogenesis of common disease are highly complicated. A genome-wide linkage study alone cannot provide the sufficient power to pinpoint the susceptibility gene. In particular, when parental information is unavailable, the power of affected sib-pair linkage analysis using microsatellite markers is low [38]. There was a report that the susceptibility gene was found in a region that showed evidence for weak linkage in a genome-wide linkage analysis [39, 40]. Further approaches such as the association study of candidate gene or a genome-wide association study using high-density single nucleotide polymorphisms are necessary.

Acknowledgments We thank OPLL patients and their families who participated in this study and the Japan OPLL Network, including Ishikawa-prefecture OPLL Tomo-no-kai. We also thank members of the Genetic Study Group of Investigation Committee on Ossification of the Spinal Ligaments. The work reported in this article was supported by a Grant for Intractable Diseases from the Public Health Bureau, the Ministry of Health and Welfare of Japan (Investigation Committee on Ossification of the Spinal Ligaments).

Conflict of interest All authors state that they have no conflicts of interest.

References

1. Stapleton CJ, Pham MH, Attenello FJ, Hsieh PC (2011) Ossification of the posterior longitudinal ligament: genetics and pathophysiology. Neurosurg Focus 30:E6
2. Matsunaga S, Sakou T (2012) Ossification of the posterior longitudinal ligament of the cervical spine: etiology and natural history. Spine 37:E309–E314
3. Saetia K, Cho D, Lee S, Kim DH, Kim SD (2011) Ossification of the posterior longitudinal ligament: a review. Neurosurg Focus 30:E1
4. Taketomi E, Sakou T, Matsunaga S, Yamaguchi M (1992) Family study of a twin with ossification of the posterior longitudinal ligament in the cervical spine. Spine 17:S55–S56
5. Matsunaga S, Sakou T (1997) Epidemiology of ossification of the posterior longitudinal ligament. In: Yonenobu K, Sakou T, Ono K (eds) Ossification of the posterior longitudinal ligament. Springer, Tokyo, pp 11–17
6. Sakou T, Matsunaga S, Koga H (2000) Recent progress in the study of pathogenesis of ossification of the posterior longitudinal ligament. J Orthop Sci 5:310–315
7. Koga H, Hayashi K, Taketomi E, Matsunaga S, Yashiki S, Fujiyoshi T, Sonoda S, Sakou T (1996) Restriction fragment length polymorphism of genes of the alpha 2(XI) collagen, bone morphogenetic protein-2, alkaline phosphatase, and tumor necrosis factor-alpha among patients with ossification of posterior longitudinal ligament and controls from the Japanese population. Spine 21:469–473
8. Tanaka T, Ikari K, Furushima K, Okada A, Tanaka H, Furukawa K, Yoshida K, Ikeda T, Ikegawa S, Hunt SC, Takeda J, Toh S, Harata S, Nakajima T, Inoue I (2003) Genomewide linkage and linkage disequilibrium analyses identify COL6A1, on chromosome 21, as the locus for ossification of the posterior longitudinal ligament of the spine. Am J Hum Genet 73:812–822
9. Nakamura I, Ikegawa S, Okawa A, Okuda S, Koshizuka Y, Kawaguchi H, Nakamura K, Koyama T, Goto S, Toguchida J, Matsushita M, Ochi T, Takaoka K, Nakamura Y (1999) Association of the human NPPS gene with ossification of the posterior longitudinal ligament of the spine (OPLL). Hum Genet 104:492–497
10. Wang H, Liu D, Yang Z, Tian B, Li J, Meng X, Wang Z, Yang H, Lin X (2008) Association of bone morphogenetic protein-2 gene

polymorphisms with susceptibility to ossification of the posterior longitudinal ligament of the spine and its severity in Chinese patients. Eur Spine J 17:956–964
11. Furushima K, Shimo-Onoda K, Maeda S, Nobukuni T, Ikari K, Koga H, Komiya S, Nakajima T, Harata S, Inoue I (2002) Large-scale screening for candidate genes of ossification of the posterior longitudinal ligament of the spine. J Bone Miner Res 17:128–137
12. Kamiya M, Harada A, Mizuno M, Iwata H, Yamada Y (2001) Association between a polymorphism of the transforming growth factor-beta1 gene and genetic susceptibility to ossification of the posterior longitudinal ligament in Japanese patients. Spine 26:1264–1266 (discussion 1266–1267)
13. Horikoshi T, Maeda K, Kawaguchi Y, Chiba K, Mori K, Koshizuka Y, Hirabayashi S, Sugimori K, Matsumoto M, Kawaguchi H, Takahashi M, Inoue H, Kimura T, Matsusue Y, Inoue I, Baba H, Nakamura K, Ikegawa S (2006) A large-scale genetic association study of ossification of the posterior longitudinal ligament of the spine. Hum Genet 119:611–616
14. Liu Y, Zhao Y, Chen Y, Shi G, Yuan W (2010) RUNX2 polymorphisms associated with OPLL and OLF in the Han population. Clin Orthop Relat Res 468:3333–3341
15. Matsunaga S, Yamaguchi M, Hayashi K, Sakou T (1999) Genetic analysis of ossification of the posterior longitudinal ligament. Spine 24:937–938
16. Numasawa T, Koga H, Ueyama K, Maeda S, Sakou T, Harata S, Leppert M, Inoue I (1999) Human retinoic X receptor beta: complete genomic sequence and mutation search for ossification of posterior longitudinal ligament of the spine. J Bone Miner Res 14:500–508
17. Kobashi G, Ohta K, Washio M, Okamoto K, Sasaki S, Yokoyama T, Miyake Y, Sakamoto N, Hata A, Tamashiro H, Inaba Y, Tanaka H (2008) FokI variant of vitamin D receptor gene and factors related to atherosclerosis associated with ossification of the posterior longitudinal ligament of the spine: a multi-hospital case–control study. Spine 33:E553–E558
18. Ogata N, Koshizuka Y, Miura T, Iwasaki M, Hosoi T, Shiraki M, Seichi A, Nakamura K, Kawaguchi H (2002) Association of bone metabolism regulatory factor gene polymorphisms with susceptibility to ossification of the posterior longitudinal ligament of the spine and its severity. Spine 27:1765–1771
19. Kim DH, Jeong YS, Chon J, Yoo SD, Kim HS, Kang SW, Chung JH, Kim KT, Yun DH (2011) Association between interleukin 15 receptor, alpha (IL15RA) polymorphism and Korean patients with ossification of the posterior longitudinal ligament. Cytokine 55:343–346
20. Chung WS, Nam DH, Jo DJ, Lee JH (2011) Association of toll-like receptor 5 gene polymorphism with susceptibility to ossification of the posterior longitudinal ligament of the spine in Korean population. J Korean Neurosurg Soc 49:8–12
21. Broman KW, Murray JC, Sheffield VC, White RL, Weber JL (1998) Comprehensive human genetic maps: individual and sex-specific variation in recombination. Am J Hum Genet 63:861–869
22. Ikari K, Onda H, Furushima K, Maeda S, Harata S, Takeda J (2001) Establishment of an optimized set of 406 microsatellite markers covering the whole genome for the Japanese population. J Hum Genet 46:207–210
23. Brownstein MJ, Carpten JD, Smith JR (1996) Modulation of non-templated nucleotide addition by Taq DNA polymerase: primer modifications that facilitate genotyping. Biotechniques 20:1004–1006, 1008–1010
24. Saito M, Saito A, Kamatani N (2002) Web-based detection of genotype errors in pedigree data. J Hum Genet 47:377–379
25. Kruglyak L, Lander ES (1995) Complete multipoint sib-pair analysis of qualitative and quantitative traits. Am J Hum Genet 57:439–454
26. Lander E, Kruglyak L (1995) Genetic dissection of complex traits: guidelines for interpreting and reporting linkage results. Nat Genet 11:241–247
27. Wu JC, Liu L, Chen YC, Huang WC, Chen TJ, Cheng H (2011) Ossification of the posterior longitudinal ligament in the cervical spine: an 11-year comprehensive national epidemiology study. Neurosurg Focus 30:E5
28. Kobashi G, Washio M, Okamoto K, Sasaki S, Yokoyama T, Miyake Y, Sakamoto N, Ohta K, Inaba Y, Tanaka H (2004) High body mass index after age 20 and diabetes mellitus are independent risk factors for ossification of the posterior longitudinal ligament of the spine in Japanese subjects: a case–control study in multiple hospitals. Spine 29:1006–1010
29. Shingyouchi Y, Nagahama A, Niida M (1996) Ligamentous ossification of the cervical spine in the late middle-aged Japanese men. Its relation to body mass index and glucose metabolism. Spine 21:2474–2478
30. Koga H, Sakou T, Taketomi E, Hayashi K, Numasawa T, Harata S, Yone K, Matsunaga S, Otterud B, Inoue I, Leppert M (1998) Genetic mapping of ossification of the posterior longitudinal ligament of the spine. Am J Hum Genet 62:1460–1467
31. Buxbaum JD, Silverman JM, Smith CJ, Kilifarski M, Reichert J, Hollander E, Lawlor BA, Fitzgerald M, Greenberg DA, Davis KL (2001) Evidence for a susceptibility gene for autism on chromosome 2 and for genetic heterogeneity. Am J Hum Genet 68:1514–1520
32. Kawaguchi H, Akune T, Ogata N, Seichi A, Takeshita K, Nakamura K (2006) Contribution of metabolic conditions to ossification of the posterior longitudinal ligament of the spine. In: Yonenobu K, Nakamura K, Toyama Y (eds) OPLL (ossification of the posterior longitudinal ligament), 2nd edn. Springer, Tokyo, pp 71–75
33. Takeuchi Y, Matsumoto T, Takuwa Y, Hoshino Y, Kurokawa T, Shibuya N, Ogata E (1989) High incidence of obesity and elevated serum immunoreactive insulin level in patients with paravertebral metabolism ligamentous ossification; a relationship to the development of ectopic ossification. J Bone Miner Metab 7:17–21
34. Nobta M, Tsukazaki T, Shibata Y, Xin C, Moriishi T, Sakano S, Shindo H, Yamaguchi A (2005) Critical regulation of bone morphogenetic protein-induced osteoblastic differentiation by Delta1/Jagged1-activated Notch1 signaling. J Biol Chem 280:15842–15848
35. Kung AW, Xiao SM, Cherny S, Li GH, Gao Y et al (2010) Association of JAG1 with bone mineral density and osteoporotic fractures: a genome-wide association study and follow-up replication studies. Am J Hum Genet 86:229–239
36. Kawaguchi H, Kurokawa T, Hoshino Y, Kawahara H, Ogata E, Matsumoto T (1992) Immunohistochemical demonstration of bone morphogenetic protein-2 and transforming growth factor-beta in the ossification of the posterior longitudinal ligament of the cervical spine. Spine 17:S33–S36
37. Tanaka H, Nagai E, Murata H, Tsubone T, Shirakura Y, Sugiyama T, Taguchi T, Kawai S (2001) Involvement of bone morphogenic protein-2 (BMP-2) in the pathological ossification process of the spinal ligament. Rheumatology 40:1163–1168
38. Evans DM, Cardon LR (2004) Guidelines for genotyping in genomewide linkage studies: single-nucleotide-polymorphism maps versus microsatellite maps. Am J Hum Genet 75:687–692
39. Onouchi Y, Gunji T, Burns JC, Shimizu C, Newburger JW et al (2008) ITPKC functional polymorphism associated with Kawasaki disease susceptibility and formation of coronary artery aneurysms. Nat Genet 40:35–42
40. Onouchi Y, Tamari M, Takahashi A, Tsunoda T, Yashiro M, Nakamura Y, Yanagawa H, Wakui K, Fukushima Y, Kawasaki T, Hata A (2007) A genomewide linkage analysis of Kawasaki disease: evidence for linkage to chromosome 12. J Hum Genet 52:179–190

Clinical Neurophysiology 125 (2014) 202–207

Contents lists available at SciVerse ScienceDirect

Clinical Neurophysiology

journal homepage: www.elsevier.com/locate/clinph

Descending spinal cord evoked potentials in cervical spondylotic myelopathy: Characteristic waveform changes seen at the lesion site

Nobuaki Tadokoro [a,*], Toshikazu Tani [a], Masahiko Ikeuchi [a], Ryuichi Takemasa [a], Kazunobu Kida [a], Tatsunori Ikemoto [b], Takahiro Ushida [c], Shinichirou Taniguchi [d], Jun Kimura [e]

[a] Department of Orthopaedic Surgery, Kochi Medical School, Japan
[b] Department of Orthopaedic Surgery, Kuroshio Hospital, Japan
[c] Multidisciplinary Pain Center, Aichi Medical School, Japan
[d] Department of Orthopaedic Surgery, Kansai Medical University Takii Hospital, Japan
[e] Department of Neurology, University of Iowa, United States

ARTICLE INFO

Article history:
Accepted 24 June 2013
Available online 24 July 2013

Keywords:
Descending spinal cord evoked potential
D-wave
Referential recording
Transcranial electrical stimulation
Conduction block

HIGHLIGHTS

- We characterized the type of D-wave changes seen at the lesion site in cervical spondylotic myelopathy with MRI evidence of single-level cord compression.
- An abrupt reduction of the negative peak accompanied by an enhancement of the initial-positive peak helps identify the site of conduction block.
- The enhancement of the positive peak tended to diminish with a more caudal compression, which may be explained by progressive loss of the descending motor volleys at the synapses in the cervical enlargement.

ABSTRACT

Objectives: To characterize waveform changes of descending spinal cord evoked potentials (D-SCEPs) seen in cervical spondylotic myelopathy (CSM).
Methods: Intraoperative D-SCEP recording from serial intervertebral discs after transcranial electrical stimulation in 19 CSM patients with cord compression at a single level.
Results: Compared to the baseline (100%) obtained one level rostrally, the D-SCEP recorded at the compression site showed a significantly ($p < 0.001$) decreased amplitude (48%) and area (48%) of negative peak and increased amplitude (171%) and area (279%) of initial-positive peak. The degree in reduction of negative peak remained the same irrespective of the cord level involved, whereas enhancement of the positive peak tended to diminish with a more caudal compression.
Conclusions: In intraoperative electrophysiological studies of CSM with D-SCEP, an abrupt reduction of the negative peak accompanied by an enhancement of the initial-positive peak helps identify the site of conduction block. We speculate that progressive loss of the descending motor volleys at the synapses in the cervical enlargement may account for limited or absent enhancement of positive peak seen caudally.
Significance: The current finding helps us understand the pros and cons of various electrophysiologic techniques for intraoperative localization of maximal cord involvement in CSM.

1. Introduction

Electrophysiologic techniques used to localize the site of the spinal cord lesion have made steady progress since earlier studies conducted under the term "electrospinogram" in animal models (Morrison et al., 1975; Rossini et al., 1980) and humans (Shimoji et al., 1971). As previously reported in cervical spondylotic myelopathy (CSM) (Tani et al., 1998, 1999, 2002), multisegmental recording of ascending spinal cord evoked potentials (A-SCEPs) can precisely localize the site of conduction abnormalities before decompression procedures. This method utilizes monopolar recording electrodes placed in the structures adjacent to the spinal cord and bipolar stimulating electrodes inserted in the lumbar epi-

* Corresponding author. Address: Department of Orthopaedic Surgery, Kochi Medical School, Kohasu Oko-chou, Nankoku 783-8505, Japan. Tel.: +81 88 880 2386; fax: +81 88 880 2388.
E-mail address: nobuaki.tadokoro@gmail.com (N. Tadokoro).

1388-2457/$36.00
http://dx.doi.org/10.1016/j.clinph.2013.06.183

dural space. An abrupt reduction in size of the negative peak accompanied by an augmentation of the initial-positive peak over a short segment serves as strong evidence of a focal conduction block. The study provided a useful addition to MRI in localizing the level of maximal cord involvement, particularly in elderly patients with clinically silent cord compression at multiple levels (Tani et al., 1999, 2002). This technique, however, has the inherent limitation of only detecting the most caudal conduction block, which precludes the evaluation of more rostral segments.

An assessment of descending spinal cord evoked potentials (D-SCEPs) after transcranial electrical stimulation (TES) of the brain, if added to A-SCEP studies, may circumvent this problem. Descending volleys in corticospinal tract axons terminate at various levels of the cord to synapse with spinal motoneurons or interneurons. This, in turn, would cause a progressive decline of motor volleys reaching the caudal recording sites, resulting in a greater diminution of the D-SCEPs than predicted from physiological temporal dispersion where the recorded potentials become smaller in amplitude and longer in duration with increasing distance between stimulating and pickup electrodes. To further clarify this relationship, we have now studied waveform changes of the D-SCEP associated with single-level cord compression. In particular, we wished to determine if the same principles of waveform changes hold for analyses of A-SCEP and D-SCEP in identifying focal conduction abnormalities.

2. Materials and methods

2.1. Patients

From January 2004 to April 2010, a total of 140 CSM patients underwent intraoperative D-SCEP studies. We selected 19 patients (11 men) ranging in age from 35 to 90 years (average, 62 years) based on MRI evidence of single-level cord compression. None had history of seizures or implanted devices such as cardiac pacemaker or cochlear implant. All agreed in writing to participate in the study after reading an informed consent form approved by the hospital ethics committee. Myelopathy resulted from cervical disc herniation in 11 and cervical spondylosis in 8 patients. All had a single-level anterior operation, 6 at C3–4 (C3–4 group), 8 at C4–5 (C4–5 group) and 5 at C5–6 (C5–6 group).

2.2. Clinical findings

The functional scale developed by the Japanese Orthopaedic Association (JOA) (Jpn Othop Assoc., 1994) scores the motor function from 0 to 4 points for both upper and lower limbs. For the upper limb, 1 patient had normal finger dexterity (4 points); 6 showed clumsy but functional writing (3 points); 8 could write but not functionally (2 points); and 4 managed to feed themselves but displayed no other function (1 point). For the lower limb, 2 patients had normal walking ability (4 points); 2 had some difficulty but were capable of fast walking unaided (3 points); 9 needed supports when going up and down the stairs (2 points); and 6 required walking aids (1 point). The combined JOA motor scores averaged 4.0 ± 1.7 (mean ± SD) for the total 19 patients and 2.4 ± 1.1 for C3–4, 4.1 ± 1.1 for C4–5, and 5.8 ± 1.3 for C5–6 group, showing a significant ($p < 0.01$) difference between C3–4 and C5–6 groups.

Muscle stretch reflexes, though generally hyperactive, showed a diminution of biceps responses in 3 patients, and of gastrocnemius–soleus in 5. Of the 5 patients with a diminished response in the gastrocnemius–soleus, 3 patients had moderate to severe radiological changes of the lumbar spine suggestive of spinal stenosis and the remaining 2 patients, either diabetes or chronic renal failure treated with regular hemodialysis. Extensor plantar responses were found in 4 patients.

2.3. MRI evaluation

All patients underwent surface coil MR examination of cervical cord preoperatively with the superconducting system (1.5 T Signa HDx; GE Healthcare, Waukesha, WI, USA). The spin echo pulse sequences were 350–600/9–12 (TR ms/TE ms) for T1- and 2600–4000/90–110 for T2-weighted images.

Cord measurements at each intervertebral level from C2–3 to C6–7 included: (1) AP-diameter on midsagittal T1-weighted images and (2) cross-sectional area on axial T1-weighted images. The values were converted into the actual diameter and area with a magnification factor. Sagittal T2-weighted images served best to detect increased signal intensity resulting from cord compression.

2.4. Stimuli

All recordings were made in the operating room of Kochi Medical School during surgery before decompression procedures. Following preoperative general anesthesia with sevoflurane, two subdermal stimulating corkscrew-like electrodes (CS001-220, A-Gram, Glenn Rock, New Jersey) were placed into the scalp 2 cm anteriorly and 5 cm laterally to the vertex on both sides (Kondo et al., 1985; Matsuda and Shimazu, 1989; Kaneko et al., 2001; Fukuoka et al., 2004; Nakanishi et al., 2006). A capacitively coupled pulse of 50 μs in duration and up to 400 V in intensity was delivered from a high-voltage electrical stimulator (Digitimer D185, Welwyn Garden City, UK) at a rate of 1/s, stimulating both sides alternately with reversed electrode polarity. Stimulus intensity was increased until a distinct D-SCEP of lowest threshold was identified.

2.5. Recording

After exposure of the anterior aspect of the vertebral bodies, a series of monopolar needle electrodes, 0.7 mm in diameter and about 4 kΩ in impedance at 1 kHz (OA210-006, Unique Medical Corp, Tokyo, Japan), were inserted into the intervertebral discs in the midline. They were then advanced posteriorly to cover the distance of the disc diameter calculated from measurement on the plain lateral radiograph. A needle electrode inserted into the skin at the caudal end of the operative field served as the common reference. This location of the reference electrode was chosen to minimize stimulus artifact. Accumulated evidence supports the validity of using a common distant reference when recording SCEPs from active leads placed equidistant to the spinal cord (Cracco and Evans, 1978; Schramm et al., 1983; Halter et al., 1989; Matsuda and Shimazu, 1989; Nakanishi et al., 2006). Also, a traveling impulse within the cervical spinal cord does not encounter a sudden geometric change of the volume conductor, which may register far-field potentials complicating recording with a referential montage. A pair of alligator clips was attached to the skin at the operative site as the ground electrode. A muscle relaxant (vecuronium, 0.015–0.110 mg/kg bolus) administered intravenously immediately before recording D-SCEP abolished interference from the twitch of paraspinal muscles near the electrodes.

The recording sites included three to five serial vertebral levels between C2–3 and C6–7 to cover the extent of vertebral exposure required for the respective decompression; three levels in 5 patients, four levels in 11 and five levels in 3. Each test set comprised an average of 50 summated potentials, sampled at 50 kHz, with a frequency response of 20 Hz–3 kHz.

An eight channel averager (Neuropak MEB2200, Nihonkohden, Tokyo, Japan) allowed simultaneous recording of D-SCEPs from all sets of electrodes. Two tracings obtained from each electrode derivation confirmed consistency. We employed low amplifier sensitivity first for digital averaging followed by optimal amplification. This arrangement circumvented the problem of a large shock artifact and amplifier overload caused by a high-voltage TES in referential recordings of the short-latency responses.

The MRI-based site of cord compression, designated as '0', served as the point of reference for the remaining levels numbered in order of increasing distance, assigning a minus sign caudally (Figs. 1–4). Measurements of D-SCEP included: (1) latencies from the stimulus artifacts to the initial positive peaks; (2) amplitudes from the baseline to the initial-positive and the negative peaks; and (3) areas (voltage–time integral) of the initial-positive and the negative phases.

2.6. Statistical analysis

We used Wilcoxon's signed rank test for evaluating paired data and one-way ANOVA followed by Games–Howell test for unpaired data. Values are given as mean ± SD and two-tailed tests were considered significant when $p < 0.05$. All statistical analyses were performed using SPSS software, version 16 (SPSS Inc., Chicago, Illinois).

3. Results

3.1. MRI

Table 1 summarizes the results of quantitative assessment of the cord compression. At '0' level, sagittal and axial T1-weighted MRI showed a significantly ($p \leqslant 0.001$) smaller anteroposterior diameter and cross-sectional area than the remaining more caudal and rostral levels. Sagittal T2-weighted MRI disclosed a high intensity spinal cord signal in all 19 patients, all at '0' level.

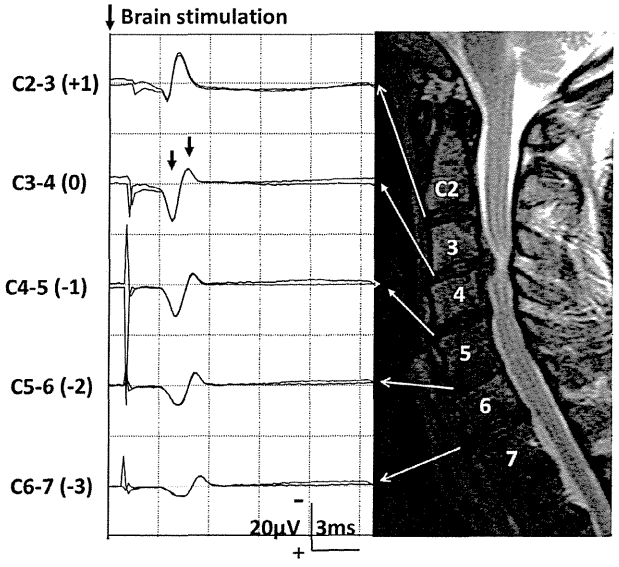

Fig. 1. A 57 year-old man with cervical spondylotic myelopathy had an isolated cord compression at C3–4 as evidenced by a sagittal T2-weighted MRI (right). Anterior recording of D-SCEPs (left) showed an abrupt reduction of negative peak to 46% in amplitude and 32% in area at this level compared to C2–3 (100%) with a concomitant augmentation of the initial-positive peak to 219% and 673% respectively. These findings indicate a partial conduction block at C3–4.

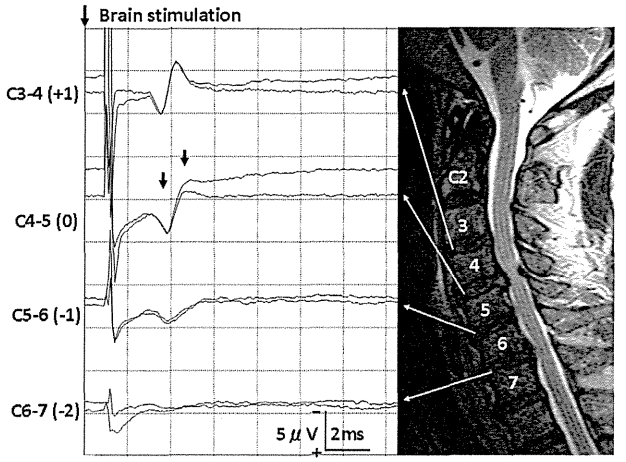

Fig. 2. A 69 year-old man with cervical spondylotic myelopathy had an isolated cord compression at C4–5 as evidenced by a sagittal T2-weighted MRI (right). Anterior recording of D-SCEPs (left) showed an abrupt reduction of negative peak to 40% in amplitude and 75% in area at this level compared to C3–4 (100%) with a concomitant augmentation of the initial-positive peak to 116% and 118% respectively. A monophasic positive wave caudally indicates a complete conduction block at C4–5.

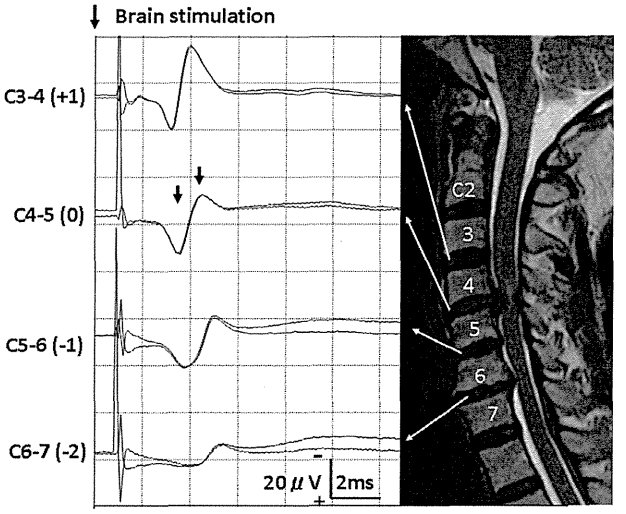

Fig. 3. A 49 year-old man with cervical spondylotic myelopathy with isolated cord compression at C4–5 as shown by a sagittal T2-weighted MRI (right). Anterior recording of D-SCEPs (left) showed an abrupt reduction of negative peak to 42% in amplitude and 29% in area at this level compared to C3–4 (100%) with a concomitant augmentation of the initial-positive peak to 108% and 189% respectively. These findings indicate a partial conduction block at C4–5.

3.2. D-SCEP

With serial recording, cortical TES delivered alternately from right and left scalp electrodes placed symmetrically consistently yielded a well-defined D-SCEP at each level of the intervertebral discs (Figs. 1–4). The potentials generally consisted of two components, the initial-positive and subsequent negative peaks. Data from the patients with a caudal lesion (C5–6 group) included: (1) onset latency of D-SCEP recorded at C4–5 (mean ± SD: 3.31 ± 0.10 ms), ranging from 3.16 to 3.42 ms ($n = 5$) and (2) conduction velocity from C3–4 to C4–5 (60.9 m/s) obtained by dividing the distance between the two recording sites (20.7 mm) by the latency difference (0.34 ms) ($n = 1$).

At the site of cord compression, or '0' level, the negative peaks showed a significantly ($p < 0.001$) reduced amplitude (48 ± 18%)

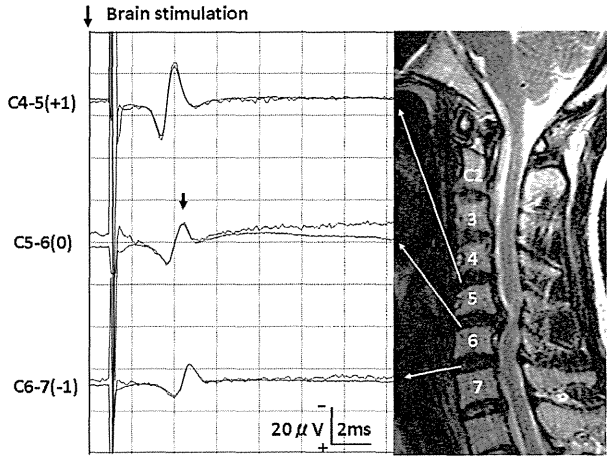

Fig. 4. A 48 year-old woman with cervical spondylotic myelopathy with isolated cord compression at C5–6 as shown by a sagittal T2-weighted MRI (right). Anterior recording of D-SCEPs (left) showed an abrupt reduction of negative peak to 42% in amplitude and 38% in area at this level compared to C4–5 (100%), indicating a partial conduction block. Unlike the cases with conduction block more rostrally (cf. Figs. 1–3), the initial-positive peak showed a distinct increase neither in amplitude (70%) nor area (102%).

Table 1
Cervical cord measurement.

Intervertebral level	Number of patients	APD[a] Mean ± SD (range) mm	CA[b] Mean ± SD (range) mm^2
+2	13	6.2 ± 0.4 (5.6–7.0)	55.4 ± 5.1 (45.1–63.9)
+1	19	6.0 ± 0.7 (4.2–7.2)	57.1 ± 6.9 (45.9–69.5)
0	19	3.8 ± 1.1* (1.5–5.6)	42.4 ± 9.7** (24.2–67.9)
−1	19	5.5 ± 0.6 (4.7–7.1)	54.5 ± 7.4 (42.8–70.3)
−2	18	5.5 ± 0.7 (4.2–6.8)	49.0 ± 8.6 (35.7–76.1)

One-way ANOVA and Games–Howell test is used for statistical analysis.
[a] APD, anteroposterior diameter measured on midsagittal T1 weighted MRI.
[b] CA, cross sectional area measured on axial T1 weighted MRI.
* Significantly smaller ($p < 0.001$) compared to more caudal and rostral levels.
** Significantly smaller ($p \leqslant 0.001$) compared to more caudal and rostral levels except for '−2'.

and area (48 ± 24%) compared to the baseline at '+1' level (100%) (Table 2). In contrast, the initial-positive peak showed a significant ($p < 0.01$) increase in amplitude (171 ± 96%) and area (279 ± 201%) at '0' level compared to '+1' (Table 3). Caudal to the site of compression, the negative peak declined further ($p < 0.01$) in amplitude (35 ± 24%) and area (32 ± 25%) at '−1', without a concomitant increase in size of the initial-positivity. A series of waveform changes indicated a complete conduction block with initial positive waves alone or abolition of any wave at points beyond the block in 6 patients (Fig. 2) and partial block in 13 patients (Figs. 1, 3 and 4). On the average, JOA motor scores (mean ± SD) for the upper and lower limbs combined showed a lower value in patients with a complete block (3.5 ± 1.7) than those with a partial block (4.3 ± 1.7), but the difference was not statistically significant ($p = 0.37$). This finding probably reflects not only the relatively small sample size but also the nature of the JOA functional assessment scale, which heavily depends on age-related disabilities not directly attributable to myelopathy.

The negative peak showed a similar size reduction (mean ± SD) at the compression site ('0') irrespective of the level involved ($p > 0.5$); its amplitude and area decreasing to 53% ± 20% ($p < 0.05$) and 49% ± 29% ($p < 0.05$) in the C3–4 group, 44% ± 21% ($p < 0.05$) and 49% ± 27% ($p < 0.05$) in the C4–5 group and 47% ± 10% ($p < 0.05$) and 45% ± 13% ($p < 0.05$) in the C5–6 group (Fig. 5A). In contrast, enhancement of the initial-positive peak at '0' level showed lesion-site dependent change: the more caudal the site of compression, the less the enhancement; its amplitude and area increasing to 227% ± 84% ($p < 0.05$) and 442% ± 212% ($p < 0.05$) in the C3–4 group, 170% ± 110% ($p > 0.05$) and 252% ± 176% ($p < 0.05$) in the C4–5 group, and 106% ± 36% ($p > 0.05$) and 126% ± 27% ($p < 0.05$) in the C5–6 group (Fig. 5B). This tendency of rostrally prominent enhancement showed a significant ($p < 0.05$) difference in area between C3–4 and C5–6 groups.

4. Discussion

In anesthetized CSM patients, high-voltage TES pulse of up to 400 V in intensity and 50 μs in duration consistently elicits a well-defined D-SCEP recordable from the cervical intervertebral discs.

A pair of scalp electrodes placed symmetrically, one on each hemisphere 5 cm from the midline, (Kondo et al., 1985; Matsuda and Shimazu, 1989; Kaneko et al., 2001; Fukuoka et al., 2004; Nakanishi et al., 2006; Tanaka et al., 2006) serve well to stimulate both sides alternately with reversed electrode polarity. This mode of stimulation with single shocks probably activates descending motor pathways to both upper and lower limbs bilaterally. In fact, 4-pulse stimulus train with an interstimulus interval of 2 ms delivered from the electrodes of the same location excited motoneurons trans-synaptically, eliciting muscle responses from hands and legs during intraoperative spinal cord monitoring in previous studies (Fukuoka et al., 2004; Tanaka et al., 2006).

This stimulation technique evoked a relatively large, synchronous D-SCEP even under inhalational anesthesia showing a short latency (3.3 ± 0.1 ms at C4–5) and fast conduction velocity (60.9 m/s), similar to those estimated for the D-wave in humans (Boyd et al., 1986; Rothwell et al., 1989, 1994; Kaneko et al., 2001; Lazzaro et al., 2004; Nakanishi et al., 2006; Lefaucheur

Table 2
Negative component of D-SCEP.

Recording level	Number of patients	Amplitude			Area		
		Mean ± SD (range), μV	Mean ± SD, %	p-Value[a]	Mean ± SD (range), μV ms	Mean ± SD, %	p-Value[a]
+1	19	14.3 ± 11.3 (3.0–53.3)	100		13.0 ± 13.0 (1.9–60.3)	100	
				<0.001			<0.001
0	19	6.1 ± 3.5 (1.4–13.3)	48 ± 18		4.5 ± 2.5 (1.4–9.3)	48 ± 24	
				0.004			0.001
−1	19	4.8 ± 4.1 (0–14.3)	35 ± 24		3.0 ± 2.4 (0–7.8)	32 ± 25	
				0.012			0.021
−2	13	1.8 ± 1.7 (0–4.4)	19 ± 14		1.6 ± 1.6 (0–4.6)	17 ± 14	

[a] Calculated according to Wilcoxon signed rank test.

Table 3
Initial-positive component of D-SCEP.

Recording level	Number of patients	Amplitude			Area		
		Mean ± SD (range), μV	Mean ± SD, %	*p*-Value[a]	Mean ± SD (range), μV ms	Mean ± SD, %	*p*-Value[a]
+1	19	6.6 ± 4.3 (0.8–14.3)	100		3.1 ± 2.3 (0.3–9.0)	100	
				0.007			<0.001
0	19	8.9 ± 5.0 (2.3–20.2)	171 ± 96		6.0 ± 3.9 (0.8–15.1)	279 ± 201	
				0.004			NS
−1	19	6.6 ± 4.4 (1.4–16.4)	135 ± 94		5.3 ± 4.4 (0.9–14.3)	265 ± 230	
				0.003			0.016
−2	13	3.1 ± 2.2 (0.7–8.0)	81 ± 51		2.8 ± 2.4 (0.2–8.2)	217 ± 184	

[a] Calculated according to Wilcoxon signed rank test.

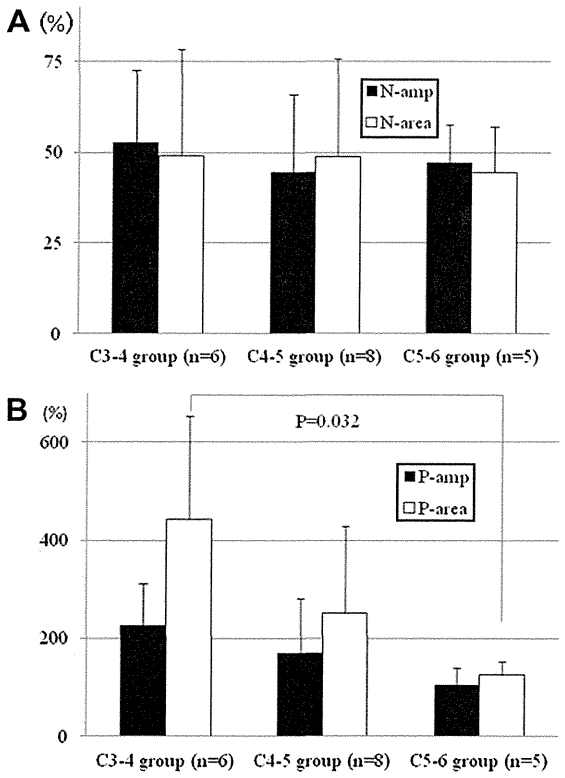

Fig. 5. (A) Graphs showing the degree of reduction in amplitude and area of the negative peak of the D-SCEP from '+1' to '0' in the three groups of patients based on the level of compression sites. Note reduction of the negative peak nearly by the same percentage irrespective of the compression level. (B) Graphs showing the degree of augmentation in amplitude and area of the initial-positive peak of the D-SCEP from '+1' to '0' in the same three groups of patients as (A). Note less enhancement of the positive peak with a conduction block seen at a more caudal site showing a significant difference in area between C3–4 and C5–6 groups ($p = 0.032$, One-way ANOVA followed by Games–Howell test).

et al., 2010; Fukaya et al., 2011). The stable, rapidly conducting, anesthesia-resistant nature of this potential also supports the contention that the D-SCEP results from the D-wave, which in animal experiments, can be recorded directly from the corticospinal tract (Patton and Amassian, 1954; Kernell and Wu, 1967) and, during human scoliosis surgeries, from the cervical epidural space (Boyd et al., 1986; Rothwell et al., 1989, 1994; Burke et al., 1990, 1992, 1995).

The D-SCEPs consisted only of a single D-wave of about 3–4 ms in onset latency without high-threshold D-wave components of shorter latency, suggesting the activation of corticospinal axons at or near the cerebral cortex (Rothwell et al., 1989, 1994; Burke et al., 1990, 1992). Therefore, it is unlikely that caudal spread of stimulating current activated the sensory tracts in the pons and brainstem, hence the D-SCEP would not be contaminated by antidromic sensory volleys. A contribution of ventral root activities to the D-SCEPs was also unlikely, because the alpha motoneurons do not reach their firing threshold with the single-pulse TES in anesthetized patients (Deletis and Sala, 2008). The D-wave was not followed by clear I-waves, probably because I-waves, compared to D-wave, are far more susceptible to inhalational anesthesia and more dispersed at modest stimulus intensities as in the present study (Rothwell et al., 1989; Burke et al., 1992).

Recording a short-latency D-SCEP using a referential derivation poses the technical challenge of eliminating amplifier overload caused by a high-voltage TES pulse of up to 400 V in intensity and 50 μs in duration. We employed a low amplifier sensitivity for the initial averaging with alternate stimulation of the right and left scalp to minimize baseline shifts caused by surface spread of stimulus current. Subsequent amplification optimal to evoke maximal D-SCEPs allowed accurate analyses of both positive and negative peaks. A bolus injection of a muscle relaxant (vecuronium, 0.015–0.110 mg/kg) immediately before the recording also helped eliminate contamination from paraspinal muscles near the recording electrodes.

In this series of CSM patients with MRI evidence of cord compression at single levels, the D-SCEP showed an abrupt reduction in size of the negative peak accompanied by an enlargement of the initial positive peak at the compression site (Figs. 1–4). These waveform changes can be explained by the concept of phase cancellation (Kimura et al., 1988), which dictates the size of a compound nerve action potential as a linear summation of the constituent nerve fiber action potentials. The overlap of the nerve fiber action potential with opposite polarity results in physiologic cancellation and reduction in the peak of compound action potentials. In the lead of compression site, a blocked fiber contributes a normal positivity followed by a substantially reduced negativity, as the impulse approaches without reaching the recording site (Woodbury, 1965; Tani et al., 1997; Kimura, 2001). This reduction in negativity not only decreases the negative peak of the D-SCEP but also increases its positive peak resulting from loss of physiological phase cancellation (Kimura et al., 1988; Tani et al., 1997, 1998, 2001). The combination of the opposing changes seen in the negative and positive peaks characterizes the D-SCEP at the compression sites, as shown in previous studies of A-SCEP in CSM patients (Tani et al., 1998, 1999, 2002).

Why then, does the initial-positive peak enhancement progressively decline with a more caudal site of conduction block, despite similar reduction of the negative peak at all levels of involvement (Fig. 5)? The long descending axons originating in the brain terminate at various levels of the cord and most abundantly at the cervical enlargement, which contains numerous motoneurons innervating the upper limbs (Kelly, 1991). Thus, progressively fewer descending axons remain caudally leading to a decreasing size of the D-SCEP with a steep change at C5–6 level. At a caudal level of conduction block, therefore, this physiological reduction of the D-SCEP adds a further decrease in size of the negative peak, at the same time countering the positive peak enhancement. In this

series, patients in the C5–6 group had a relatively mild myelopathy as indicated by a significantly higher JOA motor score compared with the C3–4 group. Therefore, a smaller degree of conduction block in the C5–6 group may also have contributed to a smaller change of the positive and negative peaks of the D-SCEP compared to the C3–4 group.

We conclude that the D-SCEP serves as a useful measure in detecting the most rostral conduction block in the motor pathways, complementing the A-SCEP used to localize the most caudal conduction block in the sensory pathways. A change in negative peak, irrespective of the level of involvement, provides a better indication of compression site at more caudal levels, where partial conduction block may not alter the initial positive peak.

Financial interest

No conflicts of interest.

References

Boyd SG, Rothwell JC, Cowan JMA, Webb RJ, Morley T, Asselman P, et al. A method of monitoring function in corticospinal pathways during scoliosis surgery with a note on motor conduction velocities. J Neurol Neurosurg Psychiatry 1986;49:251–7.

Burke D, Hicks RG, Stephen JPH. Corticospinal volleys evoked by anodal and cathodal stimulation of the human motor cortex. J Physiol 1990;425:283–90.

Burke D, Hicks R, Stephen J, Woodforth I, Crawford M. Assessment of corticospinal and somatosensory conduction simultaneously during scoliosis surgery. Electroencephalogr Clin Neurophysiol 1992;85:388–96.

Burke D, Hicks R, Stephen J, Woodforth I, Crawford M. Trial-to-trial variability of corticospinal volleys in human subjects. Electroencephalogr Clin Neurophysiol 1995;97:231–7.

Cracco RQ, Evans B. Spinal evoked potential in the cat: effects of asphyxia, strychnine, cord section and compression. Electroencephalogr Clin Neurophysiol 1978;44:187–201.

Deletis V, Sala F. Intraoperative neurophysiological monitoring of the spinal cord during spinal cord and spine surgery: a review focus on the corticospinal tracts. Clin Neurophysiol 2008;119:248–64.

Fukaya C, Sumi K, Otaka T, Shijo K, Nagaoka T, Kobayashi K, et al. Corticospinal descending direct wave elicited by subcortical stimulation. J Clin Neurophysiol 2011;28:297–301.

Fukuoka Y, Komori H, Kawabata S, Ohkubo H, Mochida K, Shinomiya K. Transcranial electrical stimulation as predictor of elicitation of intraoperative muscle-evoked potentials. Spine 2004;29:2153–7.

Halter JA, Haftek I, Sarzynska M, Dimitrijevic MR. Spinal cord evoked injury potentials in patients with acute spinal cord injury. J Neurotrauma 1989;6:231–45.

Japanese Orthopaedic Association. Scoring system (17-2) for cervical myelopathy. *Nippon Seikeigeka Gakkai Zasshi* 1994;68:498.

Kaneko K, Taguchi T, Morita H, Yonemura H, Fujimoto H, Kawai S. Mechanism of prolonged central motor conduction time in compressive cervical myelopathy. Clin Neurophysiol 2001;112:1035–40.

Kelly JP. The neural basis of perception and movement. In: Kandel ER, Schwartz JH, Jessell TM, editors. Principles of neural science. 3rd ed. Tokyo: Elsevier; 1991. p. 283–95.

Kernell D, Wu CP. Responses of the pyramidal tract to stimulation of the baboon's motor cortex. J Physiol 1967;191:653.

Kimura J, Sakimura Y, Machida M, Fuchigami Y, Ishida T, Claus D, et al. Effect of desynchronized input on compound sensory and muscle action potentials. Muscle Nerve 1988;11:694–702.

Kimura J. Electrodiagnosis in diseases of nerve and muscle: principles and practice. 3rd ed. New York: Oxford University Press; 2001. p. 27–38.

Kondo M, Matsuda H, Miyawaki Y, Yoshimura M, Shimazu A. A new method of electrodiagnosis during operations on the brachial plexus and peripheral nerve injuries. Int Ortop 1985;9:115–21.

Lazzaro VD, Oliviero A, Pilato F, Saturno E, Dileone M, Meglio M, et al. Comparison of descending volleys evoked by transcranial and epidural motor cortex stimulation in a conscious patient with bulbar pain. Clin Neurophysiol 2004;115:834–8.

Lefaucheur JP, Holsheimer J, Goujon C, Keravel Y, Nguyen JP. Descending volleys generated by efficacious epidural motor cortex stimulation in patients with chronic neuropathic pain. Exp Neurol 2010;223:609–14.

Matsuda H, Shimazu A. Intraoperative spinal cord monitoring using electric responses to stimulation of caudal spinal cord or motor cortex. In: Desmedt JE, editor. Neuromonitoring in surgery. Tokyo: Elsevier Science Publishers; 1989. p. 175–90.

Morrison G, Lorig RJ, Brodkey JS, Nulsen FE. Electrospinogram and spinal and cortical evoked potentials in experimental spinal cord trauma. J Neurosurg 1975;43:737–41.

Nakanishi K, Tanaka N, Fujiwara Y, Kamei N, Ochi M. Corticospinal tract conduction block results in the prolongation of central motor conduction time in compressive cervical myelopathy. Clin Neurophysiol 2006;117:623–7.

Patton HD, Amassian VE. Single and multiple unit analysis of cortical stage of pyramidal tract activation. J Neurophysiol 1954;17:345.

Rossini PM, Greco F, De Palma L, Pisano L. Electrospinogram of the rabbit: monitoring of the spinal conduction in acute cord lesions versus clinical observation. Eur Neurol 1980;19:409–13.

Rothwell JC, Day BL, Thompson PD, Boyd SG, Marsden CD. Motor cortical stimulation in intact man: physiological mechanisms and application in intraoperative monitoring. In: Desmedt JE, editor. Neuromonitoring in surgery. Tokyo: Elsevier Science Publishers; 1989. p. 71–98.

Rothwell J, Burke D, Hicks R, Stephen J, Woodforth I, Crawford M. Transcranial electrical stimulation of the motor cortex in man: further evidence for the site of activation. J Physiol 1994;481:243–50.

Schramm J, Krause R, Shigeno T, Brock M. Experimental investigation on the spinal cord evoked injury potential. J Neurosurg 1983;59:485–92.

Shimoji K, Higashi H, Kano T. Epidural recording of spinal electrogram in man. Electroencephalogr Clin Neurophysiol 1971;30:236–9.

Tanaka N, Nakanishi K, Fujiwara Y, Kamei N, Ochi M. Postoperative segmental C5 palsy after cervical laminoplasty may occur without intraoperative nerve injury: a prospective study with transcranial electric motor-evoked potentials. Spine 2006;31:3013–7.

Tani T, Ushida T, Yamamoto H, Okuhara Y. Waveform changes due to conduction block and their underlying mechanism in spinal somatosensory evoked potential: a computer simulation. J Neurosurg 1997;86:303–10.

Tani T, Ushida T, Yamamoto H, Kimura J. Waveform analysis of spinal somatosensory evoked potential: paradoxically enhanced negative peak immediately caudal to the site of conduction block. Electroencephalogr Clin Neurophysiol 1998;108:325–30.

Tani T, Yamamoto H, Kimura J. Cervical spondylotic myelopathy in elderly people: a high incidence of conduction block at C3–4 or C4–5. J Neurol Neurosurg Psychiatry 1999;66:456–64.

Tani T, Ushida T, Kimura J. Sequential changes of orthodromic sensory nerve action potentials induced by experimental compression of the median nerve at the wrist. Clin Neurophysiol 2001;112:136–44.

Tani T, Ushida T, Taniguchi S, Kimura J. Age related shift in the primary sites of involvement in cervical spondylotic myelopathy from lower to upper levels. J Neurol Neurosurg Psychiatry 2002;73:316–8.

Woodbury JW. Potentials in a volume conductor. In: Ruch TC, Patton HD, Woodbury JW, Towe AL, editors. Neurophysiology. 2nd ed. Philadelphia: W.B. Saunders; 1965. p. 85–91.